# Prototype Sandia Octahedral Molecular Sieve (SOMS) $Na_2Nb_2O_6 \cdot H_2O$: Synthesis, Structure and Thermodynamic Stability

Hongwu Xu,*,† May Nyman,‡ Tina M. Nenoff,‡ and Alexandra Navrotsky†

*Thermochemistry Facility and NEAT ORU, University of California at Davis, Davis, California 95616 and Sandia National Laboratories, P.O. Box 5800, M.S. 0755, Albuquerque, New Mexico 87185*

*Received October 24, 2003. Revised Manuscript Received March 3, 2004*

A new microporous phase $Na_2Nb_2O_6 \cdot H_2O$, which transforms to $NaNbO_3$ perovskite on heating, has been synthesized by the hydrothermal method. Rietveld analysis of powder synchrotron X-ray diffraction data reveals that the structure comprises a framework of $[NbO_6]$ and $[NaO_6]$ octahedra with other $Na^+$ being located in the channels (space group $C2/c$; $a$ = 17.0511(9) Å; $b$ = 5.0293(2) Å; $c$ = 16.4921(9) Å; $\beta$ =113.942(2)°). This phase belongs to the recently synthesized Sandia octahedral molecular sieves (SOMS) family, $Na_2Nb_{2-x}M_xO_{6-x}(OH)_x \cdot H_2O$ (M = Ti, Zr) and is the archetype for the substituted structures. Using drop-solution calorimetry into molten $3Na_2O \cdot 4MoO_3$ at 974 K, the enthalpies of formation of $Na_2Nb_2O_6 \cdot H_2O$ from the constituent oxides and from the elements have been determined to be $-295.4 \pm 4.8$ and $-2895.5 \pm 6.4$ kJ/mol, respectively. From the drop-solution calorimetric data for $Na_2Nb_2O_6 \cdot H_2O$ and its dehydrated perovskite phase, the enthalpy of the dehydration reaction, $Na_2Nb_2O_6 \cdot H_2O \rightarrow 2NaNbO_3 + H_2O$, has been derived, and its implications for phase stability are discussed.

## Introduction

In the past decades, microporous framework materials composed of octahedral units (such as $[TiO_6]$) have attracted much attention due to their unique properties compared to those of conventional zeolitic phases whose frameworks consist of $[SiO_4]$ and $[AlO_4]$ tetrahedra.[1,2] More recently, Nyman et al.[3,4] and Nenoff and Nyman[5] synthesized a new class of octahedral microporous phases with the compositions $Na_2Nb_{2-x}M_xO_{6-x}(OH)_x \cdot H_2O$ (M = Ti, Zr; $0 < x \leq 0.4$) using hydrothermal methods. These phases, named Sandia octahedral molecular sieves (SOMS), possess a framework structure composed of $[NbO_6]$, $[MO_6]$, and $[NaO_6]$ octahedra linked by corner- or edge-sharing. In the structure, Nb and Ti/Zr occupy the same framework positions, and the remaining Na resides in the channels. This structure is unusual in the sense that Na, which is typically an extraframework cation, also participates in the formation of the framework. Ion exchange experiments show that the SOMS phases are highly selective for large alkaline earth cations over alkali cations. For example, the distribution coefficient ($K_d$), which is defined as the ratio of cation adsorbed onto the ion exchanger to the cation remaining in the solution, for the $Na_2Nb_{0.6}Ti_{0.4}O_{5.6}(OH)_{0.4} \cdot H_2O$ phase is about $10^5$ for $Sr^{2+}$, but only 95 for $K^+$.[3] Hence, these materials can potentially be used for separation of radioactive $^{90}Sr$ from aqueous nuclear wastes and contaminated groundwater. Moreover, upon heating, the Sr-exchanged SOMS phases dehydrate and convert to thermally stable and chemically durable perovskites.[4] Thus, these perovskites may serve as permanent ceramic host phases for $^{90}Sr$ in radioactive waste management.

As Ti or Zr occupies the same sites as Nb in the framework, the $Na_2Nb_{2-x}M_xO_{6-x}(OH)_x \cdot H_2O$ phases can be considered as derivatives of the nominal $Na_2Nb_2O_6 \cdot H_2O$ structure through the following substitution: $M^{4+} + OH^- \rightarrow Nb^{5+} + O^{2-}$. However, the end-member phase containing only Nb without Ti or Zr with the nominal composition $Na_2Nb_2O_6 \cdot H_2O$ has not previously been synthesized. The instability of this phase compared to its related perovskite $NaNbO_3$ rendered its synthesis more challenging than that of the Ti- and Zr-substituted compositions. We present here the synthesis of this prototypic phase using the hydrothermal method. Rietveld analysis of powder synchrotron X-ray diffraction (XRD) data reveals that it adopts the same type of framework topology as the Ti- or Zr-substituted phases. The absence of $OH^-$ and of cation substitution in this phase makes it ideal for investigating the structural characteristics of this new framework type. Moreover, the enthalpies of formation of $Na_2Nb_2O_6 \cdot H_2O$ from the oxides and from the elements have been determined using drop-solution calorimetry with $3Na_2O \cdot 4MoO_3$ as

* To whom correspondence should be addressed. Phone: 530-754-2132. Fax: 530-752-9307. E-mail: hxu@ucdavis.edu.
† University of California at Davis.
‡ Sandia National Laboratories.

(1) Anderson, M. W.; Terasaki, O.; Ohsuna, T.; Malley, P. J. O.; Philippou, A.; MacKay, S. P.; Ferreira, A.; Rocha, J.; Lidin, S. *Philos. Mag. B* **1995**, *71*, 813.
(2) Clearfield, A. *Solid State Sci.* **2001**, *3*, 103.
(3) Nyman, M.; Tripathi, A.; Parise, J. B.; Maxwell, R. S.; Harrison, W. T. A.; Nenoff, T. M. *J. Am. Chem. Soc.* **2001**, *123*, 1529.
(4) Nyman, M.; Tripathi, A.; Parise, J. B.; Maxwell, R. S.; Nenoff, T. M. *J. Am. Chem. Soc.* **2002**, *124*, 1704.
(5) Nenoff, T.; Nyman, M. A New Class of Inorganic Molecular Sieves: Sodium Niobium Metal Oxides. U.S. Patent (submitted), 2001.

10.1021/cm035066i CCC: $27.50 
Published on Web 04/15/2004

solvent at 974 K. From the measured heats of drop solution of $Na_2Nb_2O_6 \cdot H_2O$ and its dehydrated microporous and perovskite phases, the enthalpies of the dehydration reactions, $Na_2Nb_2O_6 \cdot H_2O \rightarrow Na_2Nb_2O_6$ (microporous) + $H_2O$ and $Na_2Nb_2O_6 \cdot H_2O \rightarrow 2NaNbO_3$ (perovskite) + $H_2O$ at room temperature have been obtained, and the stability relations among the three phases are discussed.

## Experimental Methods

**Sample Synthesis.** $Na_2Nb_2O_6 \cdot H_2O$ was prepared via a hydrothermal route. Pentaethoxyl niobium $Nb(OEt)_5$ (2.8 mmol) was put into a 20-mL glass vial in an inert atmosphere box. The vial was capped and then removed from the drybox. Sodium hydroxide (1.34 g, 33.6 mmol) was dissolved in 8 mL of deionized water in a 23-mL Teflon liner for a pressurized Parr reactor vessel. While the NaOH solution was being stirred, $Nb(OEt)_5$ was added and the solution was stirred for 30 min more. The final ratio of $Na/Nb/H_2O$ was 12:1:159, and the final pH of the solution was around 13.7. The Teflon liner containing the aqueous mixture was placed inside the steel pressure reactor, and the whole assembly was then placed in an oven and heated at 448 K for 4 h. More extensive heating led to conversion of the microporous phase to $NaNbO_3$ perovskite. The yield was approximately 0.4 g, or 90% yield based on the metal alkoxides.

**Powder synchrotron X-ray diffraction and Rietveld refinement.** Powder synchrotron XRD measurements of $Na_2Nb_2O_6 \cdot H_2O$ were performed with a linear position-sensitive detector (PSD) at beam line X7A[6] of the National Synchrotron Light Source, Brookhaven National Laboratory. The wavelength used is 0.72580 Å, as calibrated using a $CeO_2$ standard. Powders of $Na_2Nb_2O_6 \cdot H_2O$ were sealed in a glass capillary 0.6-mm in diameter, and, to minimize preferred orientation, the capillary was fully rotated during data collection. Data were collected from 5° to 60° $2\theta$ in step-scan mode using steps of 0.25° with counting times of 10 s (5−15°), 20 s (15−30°), 40 s (30−45°), and 80 s (45−60°) per step.

The Rietveld method[7] was used to analyze the synchrotron X-ray data with the general structure analysis system (GSAS) program of Larson and Von Dreele.[8] The starting structural parameters were taken from the study of $Na_2Nb_{0.6}Ti_{0.4}O_{5.6}(OH)_{0.4} \cdot H_2O$,[3] and the refinements proceeded as follows. After the scale factor and four background terms (shifted Chebyshev function) had converged, specimen displacement and lattice parameters were added and optimized. Sixteen additional background terms were then added, and the peak profiles were fitted to pseudo-Voigt convolution functions with a peak asymmetry correction.[9,10] In addition, Debye−Scherrer absorption correction was applied. On convergence of the preceding parameters, atomic coordinates and isotropic temperature factors for Na, Nb, and O were refined. The final refinement indices are $R_{wp} = 3.6\%$, $R_p = 3.3\%$, and $R_F = 1.4\%$. The fitted pattern is plotted in Figure 1.

**NMR Spectroscopy.** The $^{23}Na$ magic angle spinning−nuclear magnetic resonance (MAS NMR) spectrum of $Na_2Nb_2O_6 \cdot H_2O$ was acquired with a Chemagnetics CMX-400 spectrometer operating at 105.836 MHz. Sample powders were held in a zirconia rotor (with an outside diameter of 4 mm) spinning at 16 kHz. Single pulses of 1.8 $\mu$s with a recycle delay of 0.5 s were used for excitation. Chemical shifts were referenced to 0.2 M NaCl solution.

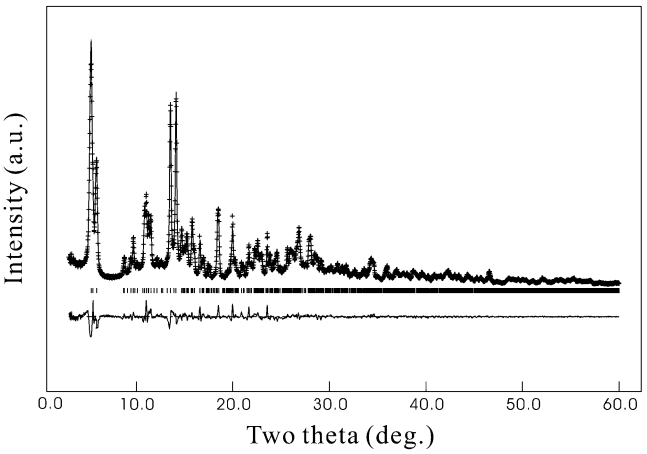


**Figure 1.** Fitted synchrotron XRD pattern of $Na_2Nb_2O_6 \cdot H_2O$. Data are shown as plus signs, and the solid curve is the best fit to the data. Tick marks below the pattern show the positions of allowed reflections, and the lower curve represents the difference between the observed and calculated profiles.

**Thermal Analysis.** Although there is one mole of water per $Na_2Nb_2O_6 \cdot H_2O$ formula, the sample usually contains additional, adsorbed surface water. The measurement of water content is important for accurate determination of the enthalpies of formation (see below). To measure the water content of our synthesized sample, and also to examine its structural evolution on increasing temperature, thermogravimetry (TG) and differential scanning calorimetry (DSC) were conducted using the Netzsch simultaneous thermal analyzer (STA) 449 system. About 25 mg of the sample powders were packed in a standardized Pt crucible. The loaded crucible was then placed into the calorimeter and heated to 1173 K with a rate of 10 K/min. For baseline correction, an earlier scan using the empty Pt crucible was run under the same conditions. Temperature was calibrated against the melting points of several metal standards (In, Bi, Zn, Al, and Au), and sensitivity calibration was done using the heat capacities of sapphire. In addition, to identify and characterize the dehydrated phase recovered from the TG/DSC scan, powder XRD was performed with a Scintag Pad-V diffractometer using Cu K$\alpha$ radiation.

**High-Temperature Drop-Solution Calorimetry.** High-temperature calorimetric measurements were performed using a Tian-Calvet microcalorimeter operating at 974 K with molten sodium molybdate ($3Na_2O \cdot 4MoO_3$) as the solvent. $Na_2Nb_2O_6 \cdot H_2O$ and its dehydrated microporous ($Na_2Nb_2O_6$) and perovskite ($NaNbO_3$) phases were measured. The instrument and experimental procedures have been described in detail by Navrotsky.[11] A sample pellet weighing ~5 mg was dropped from room temperature into the solvent in the hot calorimeter. The enthalpy measured includes the energy associated with heating the sample from room temperature to 974 K (heat content) plus the enthalpy of solution of the sample. To facilitate dissolution of the sample pellet, oxygen gas was bubbled through the solvent at a rate of ~5 $cm^3$/min. In addition, oxygen gas was flowed through the calorimeter at a rate of ~70 $cm^3$/min to sweep the bubbled oxygen and the evolved water vapor from the $Na_2Nb_2O_6 \cdot H_2O$ sample out of the calorimeter.[12] The calorimeter was calibrated against the known heat contents of corundum pellets weighing ~5 mg. Seven sample pellets each were dropped for $Na_2Nb_2O_6 \cdot H_2O$ and $NaNbO_3$ perovskite, and four pellets were dropped for the dehydrated microporous phase $Na_2Nb_2O_6$.

## Results and Discussion

**Crystal Structure.** The unit-cell parameters, atomic positions, and atomic thermal parameters of

(6) Cox, D. E.; Toby, B. H.; Eddy, M. M. *Aust. J. Phys.* **1988**, *41*, 117.
(7) Rietveld, H. M. *Acta Crystallogr.* **1967**, *22*, 151.
(8) Larson, A. C.; Von Dreele, R. B. *GSAS, General Structure Analysis System*; Report No. LAUR 86-748; Los Alamos National Laboratory: Los Alamos, NM, 2000.
(9) Thompson, P.; Cox, D. E.; Hastings, J. *J. Appl. Crystallogr.* **1987**, *20*, 79.
(10) Finger, L. W.; Cox, D. E.; Jephcoat, A. P. *J. Appl. Crystallogr.* **1994**, *27*, 892.
(11) Navrotsky, A. *Phys. Chem. Miner.* **1997**, *24*, 222.
(12) Navrotsky, A.; Rapp, R. P.; Smelik, E.; Burnly, P.; Circone, S.; Chai, L.; Bose, K.; Westrich, H. R. *Am. Mineral.* **1994**, *79*, 1099.

**Table 1. Atomic Coordinates and Isotropic Temperature Factors of $Na_2Nb_2O_6 \cdot H_2O$ (space group *C*2/*c*, cell parameters: *a* = 17.0511(9) Å; *b* = 5.0293(2) Å; *c* = 16.4921(9) Å; *β* =113.942(2)°)**

| atom | *x* | *y* | *z* | *U* (Å²/100) |
|---|---|---|---|---|
| Na(1) | 0.3347(5) | −0.3662(11) | 0.7337(5) | 1.4(1) |
| Na(2) | 0.5 | 0.1399(18) | 0.75 | 1.3(2) |
| Na(3) | 0.2628(13) | 0.2876(35) | 0.0121(12) | 2.2(4) |
| Nb(1) | 0.4052(1) | 0.0456(4) | 0.9057(1) | 0.9(1) |
| Nb(2) | 0.5325(1) | 0.5494(4) | 0.9149(1) | 1.0(1) |
| O(1) | 0.4615(5) | −0.2541(19) | −0.0039(7) | 1.0(2) |
| O(2) | 0.4773(7) | −0.1478(17) | 0.8490(8) | 1.1(2) |
| O(3) | 0.4201(7) | 0.3588(19) | 0.8500(7) | 1.1(2) |
| O(4) | 0.3777(6) | 0.2492(19) | 0.9930(6) | 1.0(2) |
| O(5) | 0.6005(6) | 0.4178(18) | 0.8607(6) | 1.6(2) |
| O(6) | 0.3018(6) | −0.0937(19) | 0.8374(7) | 1.5(2) |
| O(W) | 0.1993(7) | 0.5054(20) | 0.8687(7) | 1.8(2) |

**Table 2. Selected Bond Lengths (Å) of $Na_2Nb_2O_6 \cdot H_2O$**

| | | | |
|---|---|---|---|
| Na(3) site | | Nb(1)$O_6$ octahedron | |
| Na(3)−O(4) | 2.12(2) | Nb1−O1 | 2.06(1) |
| Na(3)−O(4) | 2.37(2) | Nb1−O1 | 2.43(1) |
| Na(3)−O(W) | 2.43(2) | Nb1−O2 | 2.07(1) |
| Na(3)−O(W) | 2.33(2) | Nb1−O3 | 1.89(1) |
| Na(3)−O(5) | 2.84(2) | Nb1−O4 | 1.97(1) |
| | | Nb1−O6 | 1.81(1) |
| Na(1)$O_6$ octahedron | | Nb(2)$O_6$ octahedron | |
| Na(1)−O(2) | 2.64(1) | Nb2−O1 | 2.36(1) |
| Na(1)−O(3) | 2.33(1) | Nb2−O1 | 2.06(1) |
| Na(1)−O(5) | 2.49(1) | Nb2−O2 | 1.89(1) |
| Na(1)−O(6) | 2.43(1) | Nb2−O3 | 2.02(1) |
| Na(1)−O(6) | 2.43(1) | Nb2−O4 | 1.95(1) |
| Na(1)−O(W) | 2.43(1) | Nb2−O5 | 1.85(1) |
| Na(2)$O_6$ octahedron | | | |
| Na(2)−O(2)[a] | 2.33(1) | | |
| Na(2)−O(3)[a] | 2.76(1) | | |
| Na(2)−O(5)[a] | 2.38(1) | | |

[a] There are two Na−O bonds with this length.

$Na_2Nb_2O_6 \cdot H_2O$ obtained from Rietveld analysis are given in Table 1, and selected bond lengths are listed in Table 2. As shown in Figure 2, the framework is composed of [$NbO_6$] and [$NaO_6$] octahedra with the remaining Na occupying the channel sites. [$NbO_6$] octahedra are connected to form double chains that run parallel to [010], whereas [$NaO_6$] are connected into layers parallel to (001), both via edge sharing. The [$NaO_6$] layers alternate with the layers containing [$NbO_6$] double chains along the *c*-axis, forming a three-dimensional network. Both [$NbO_6$] and [$NaO_6$] octahedra are irregular, as reflected by the relatively large ranges of their six Nb−O or Na−O bond distances (Table 2). These distortions may be due to the edge sharing (versus corner sharing that commonly occurs in framework structures) of [$NbO_6$] or [$NaO_6$] octahedra and the minimization of the mismatch between [$NbO_6$] and [$NaO_6$] layers. For instance, the O−O edges that are shared by two [$NbO_6$] or [$NaO_6$] octahedra tend to be shorter due to the minimization of adjacent $Nb^{5+}$ or $Na^+$ repulsion. In addition, [$NaO_6$] octahedra are presumably more flexible than [$NbO_6$], resulting in larger deviations of the bond angles O−Na−O from 90° or 180°, as would be seen in a perfect octahedron, than those of O−Nb−O (e.g., the smallest O−Na−O is 64.3°, whereas the smallest O−Nb−O is 74.8°). The extraframework Na [Na(3)] resides in the one-dimensional structural channels parallel to the *b*-axis and is coordinated to four O atoms in a distorted, square-planar geometry. Another O is 2.84 Å from Na(3) and might also be considered bonded to Na(3). More specifically, Na(3) occupies one of the two sites displaced from the center of the rectangle, rather than the center itself. Thus each Na(3) site has an occupancy of 50%. This structure is unique in the sense that Na, typically an extraframework cation, also participates in the formation of the framework. Similar structural features have been observed in some lithosilicate zeolites in which both framework and extraframework Li cations occur,[13] though in that case the framework consists of tetrahedra.

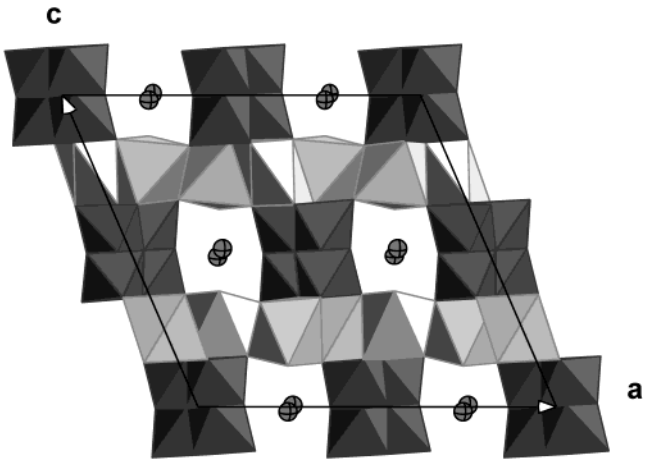


**Figure 2.** Crystal structure of $Na_2Nb_2O_6 \cdot H_2O$ projected down [010]. Black octahedra represent [$NbO_6$] units, gray octahedra represent [$NaO_6$] octahedra, and spheres represent Na ions. Solid lines outline the unit cell.

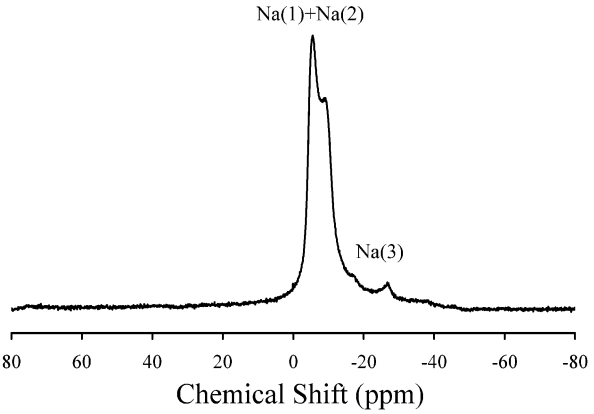


**Figure 3.** $^{23}Na$ MAS NMR spectrum of $Na_2Nb_2O_6 \cdot H_2O$.

The two types of Na sites (framework and extraframework) can be distinguished by $^{23}Na$ MAS NMR spectroscopy (Figure 3). Because of the quadrupolar effect for $^{23}Na$ and the irregularity of [Na(1)$O_6$], [Na(2)$O_6$], and [Na(3)$O_4$] polyhedra, described above, each Na site exhibits a "powder" pattern with multiple signals, rather than a single, symmetric peak. The pattern with peaks at about −5.8 and −9.0 ppm may be assigned to the two overlapping resonances from framework Na(1) and Na(2), whereas the broader pattern with singularities at about −16.8 and −27.0 ppm may be assigned to extraframework Na(3). Because the local bonding environments of Na(1) and Na(2) are only slightly different [Na(1) is bonded to five framework oxygens and one

(13) Park, S. H.; Parise, J. B.; Gies, H.; Liu, H.; Grey, C. P.; Toby, B. H. *J. Am. Chem. Soc.* **2000**, *122*, 11023.

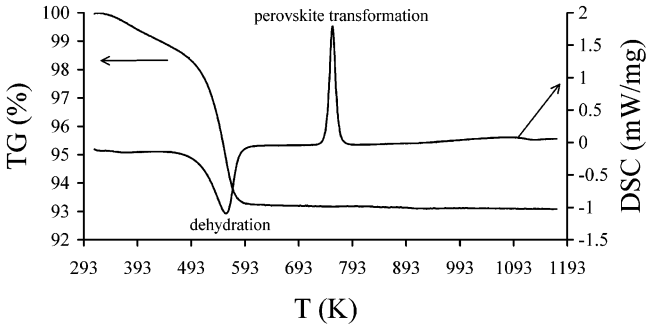


**Figure 4.** TG and DSC profiles of $Na_2Nb_2O_6 \cdot H_2O$.

water oxygen, and Na(2) is bonded to six framework oxygens], their resonances cannot be resolved in Figure 3. Nevertheless, compared to the Ti-substituted phases $Na_2Nb_{2-x}Ti_xO_{6-x}(OH)_x \cdot H_2O$ ($x = 0.04$ and 0.4),[4] $Na_2Nb_2O_6 \cdot H_2O$ shows more distinct peaks. This behavior may be attributed to the absence of Ti/Nb disorder in the structure of this end member. Specifically, in $Na_2Nb_{2-x}Ti_xO_{6-x}(OH)_x \cdot H_2O$, there exist differences, among Nb/Ti sites, in the Nb/Ti−O distances and in the number of next-nearest Ti atoms. This disordered arrangement of Nb/Ti may result in a distribution of the chemical shifts and quadrupolar interactions of the Na cations, in each of the Na sites, accounting for the broader patterns for the Ti-substituted phases.

It is noted that in the above X-ray structure refinements, we did not attempt to determine the positions of H atoms in $Na_2Nb_2O_6 \cdot H_2O$, as hydrogen is a weak X-ray scatterer. To locate the H atoms, we performed time-of-flight neutron diffraction experiments using the high-pressure preferred orientation (HIPPO) diffractometer at the Manuel Lujan, Jr. Neutron Scattering Center, Los Alamos National Laboratory. Difference Fourier maps from Rietveld analysis of the neutron data, however, reveal no distinct nuclear-density maxima corresponding to hydrogen. This implies that each H atom may be disordered over several positions, rather than occupying a single site, as seen in some zeolites such as $ND_4$-exchanged barrerite.[14] In other words, an orientation disorder of water molecules may occur in the $Na_2Nb_2O_6 \cdot H_2O$ channels, where the H atoms interact weakly with framework O via hydrogen bonding. On the other hand, as the diffraction peaks of our neutron pattern are relatively weak, presumably due to the large absorption of neutrons by hydrogen, we cannot rule out the possibility of an ordered distribution of hydrogen. To obtain a more decisive conclusion, further neutron experiments using a deuterated sample need to be conducted.

**Thermal Behavior.** Figure 4 shows the DSC/TG curves for $Na_2Nb_2O_6 \cdot H_2O$ in the temperature range 313−1173 K. With increasing temperature, $Na_2Nb_2O_6 \cdot H_2O$ showed an endothermic peak around 563 K due to the loss of its water. The corresponding weight loss is ∼6.8%. This value is higher than the ideal 5.2%, based on the formula $Na_2Nb_2O_6 \cdot H_2O$, and we attribute the additional weight loss to the removal of physically adsorbed water. On further increasing temperature, an exothermic peak appeared at ∼755 K, which arises from the transformation of microporous $Na_2Nb_2O_6$ to its dense form. XRD analysis indicates that the dense phase, recovered from the DSC/TG experiment, is $NaNbO_3$ perovskite (space group *Pbma*) with cell parameters $a = 5.5741(2)$ Å, $b = 15.5251(4)$ Å, and $c = 5.5170(2)$ Å.

**Table 3. Heat of Drop Solution of $Na_2Nb_2O_6 \cdot 1.32H_2O$ in Sodium Molybdate at 974 K**

| mass (mg) | $\Delta H_{ds}$ (kJ/mol) |
|---|---|
| 5.06 | 262.3 |
| 5.55 | 259.4 |
| 6.0 | 263.4 |
| 5.61 | 261.0 |
| 5.30 | 264.7 |
| 5.58 | 260.4 |
| 5.17 | 255.8 |
| average | 261.0 ± 2.2[a] |

[a] Uncertainty is two standard deviations of the mean.

Compared to most aluminosilicate and titanosilicate zeolites, $Na_2Nb_2O_6 \cdot H_2O$ exhibits fewer thermal events on increasing temperature. Upon heating, zeolites typically display a series of DSC peaks due to dehydration, dehydroxylation, amorphization, and recrystallization. In contrast, $Na_2Nb_2O_6 \cdot H_2O$ shows no peaks corresponding to the collapse of the sodium niobate framework (amorphization) and then its recrystallization into a denser structure. Rather, this microporous phase, after full dehydration, converts directly to the dense $NaNbO_3$ perovskite. Similar behavior has previously been seen in the Ti-substituted SOMS, $Na_2Nb_{0.6}Ti_{0.4}O_{5.6}(OH)_{0.4} \cdot H_2O$.[4]

The absence of amorphization during the thermal evolution of $Na_2Nb_2O_6 \cdot H_2O$ implies that the vitreous form of $NaNbO_3$ is energetically very unfavorable. Unlike the common glass-forming elements such as Si and B, Nb is octahedrally, rather than tetrahedrally, coordinated to oxygens, resulting in the weaker Nb−O framework structure and the apparent inability to form a glass. In fact, a previous attempt to synthesize the $NaNbO_3$ glass was unsuccessful, even with the twin-roller technique that can achieve higher quenching rates.[15] Hence, the dehydrated microporous phase $Na_2Nb_2O_6$ transforms directly to the dense $NaNbO_3$ perovskite, rather than forming an intermediate amorphous phase. Integration of the DSC curve from 713 to 793 K yields a transition enthalpy of $-28.9 \pm 2.2$ kJ per mole of $Na_2Nb_2O_6$. Because the bonding configurations of the two polymorphs are very different (for instance, Na cations in the microporous phase are coordinated to either 6 or 4 oxygens, whereas those in the perovskite are 8- or 9-coordinated), this transition has a relatively large enthalpy and is reconstructive in nature.

**Thermochemistry.** The heats of drop solution ($\Delta H_{ds}$) for seven as-synthesized sample pellets in the sodium molybdate solvent at 974 K are listed in Table 3. The averaged $\Delta H_{ds}$ is 261.0 ± 2.2 kJ/mol. As the sample contains ∼1.6 wt % adsorbed water, to obtain the $\Delta H_{ds}$ for $Na_2Nb_2O_6 \cdot H_2O$, a correction is needed. Subtraction of the heat content of the ∼1.6 wt % water from 298 to 974 K yields a $\Delta H_{ds}$ value of 238.7 ± 2.2 kJ/mol for $Na_2Nb_2O_6 \cdot H_2O$ (Table 4).

(14) Meneghinello, E.; Albert, A.; Cruciani, G.; Sacerdoti, M.; McIntyre, G.; Ciambelli, P.; Rapacciuolo, M. T. *Eur. J. Mineral.* **2000**, *12*, 1123.

(15) Nassau, K.; Wang, C. A.; Grasso, M. *J. Am. Ceram. Soc.* **1979**, *62*, 503.

**Table 4. Heats of Drop Solution in Sodium Molybdate at 974 K and Enthalpies of Formation from the Oxides and from the Elements at 298 K of $Na_2Nb_2O_6 \cdot H_2O$ and its Dehydrated Microporous ($Na_2Nb_2O_6$) and Perovskite ($NaNbO_3$) Phases**

| | $\Delta H_{ds}$ (kJ/mol)[a] | $\Delta H_{f,ox}^0$ (kJ/mol) | $\Delta H_{f,el}^0$ (kJ/mol) |
|---|---|---|---|
| $Na_2Nb_2O_6 \cdot H_2O$ | 238.7 ± 2.2 (7) | −295.4 ± 4.8 | −2895.5 ± 6.4 |
| $Na_2Nb_2O_6$ | 123.6 ± 2.8 (4) | −249.2 ± 5.1 | −2563.5 ± 6.7 |
| $NaNbO_3$ | 95.5 ± 0.8 (7) | −158.3 ± 2.3 | −1315.5 ± 3.1 |

[a] Uncertainty is two standard deviations of the mean; value in () is the number of experiments.

**Table 5. Enthalpies of Drop Solution in Sodium Molybdate at 974 K and Enthalpies of Formation from Elements at 298 K of the Oxides Used in Formation Enthalpy Calculations**

| oxide | $Na_2O$ | $Nb_2O_5$ | $H_2O$ |
|---|---|---|---|
| $\Delta H_{ds}$ (kJ/mol) | −217.56 ± 4.25[a] | 91.97 ± 0.78[b] | 68.9[c,d] |
| $\Delta H_{f,el}^0$ (kJ/mol) | −414.8 ± 0.3[d] | −1899.5 ± 4.2[e] | −285.8 ± 0.1[d] |

[a] From ref 16. [b] From ref 17. [c] Heat content from 298 to 974 K. [d] From ref 18. [e] From ref 19.

Using the above calorimetric datum, the enthalpies of drop solution and the enthalpies of formation from the elements for $Na_2O$, $Nb_2O_5$, and $H_2O$ (Table 5),[16−19] we calculated the standard molar enthalpies of formation of $Na_2Nb_2O_6 \cdot H_2O$ from the constituent oxides ($\Delta H_{f,ox}^0$) and from the elements ($\Delta H_{f,el}^0$) via the thermochemical cycles shown in Table 6. The obtained $\Delta H_{f,ox}^0$ and $\Delta H_{f,el}^0$ are −295.4 ± 4.8 kJ/mol and −2895.5 ± 6.4 kJ/mol, respectively (Table 4).

To study the stability relations between $Na_2Nb_2O_6 \cdot H_2O$ and its dehydrated microporous and perovskite phases, we also measured the $\Delta H_{ds}$ for the two anhydrous phases in molten sodium molybdate at 974 K. The perovskite phase was recovered from the DSC/TG experiment, and the dehydrated microporous sample was obtained by heating $Na_2Nb_2O_6 \cdot H_2O$ at 623 K for 2 h. The measured $\Delta H_{ds}$ values for $Na_2Nb_2O_6$ microporous phase and $NaNbO_3$ perovskite are 123.6 ± 2.8 and 95.5 ± 0.8 kJ/mol, respectively (Table 4). From these values and using appropriate thermodynamic cycles, the $\Delta H_{f,ox}^0$ and $\Delta H_{f,el}^0$ of microporous $Na_2Nb_2O_6$ are determined to be −249.2 ± 5.1 kJ/mol and −2563.5 ± 6.7 kJ/mol, respectively, and those for $NaNbO_3$ perovskite are −158.3 ± 2.3 kJ/mol and −1315.5 ± 3.1 kJ/mol, respectively (Table 4). The formation enthalpies for $NaNbO_3$ perovskite are in excellent agreement with those reported previously, even though the sample used in the earlier study was prepared by the sol−gel method.[20]

From the $\Delta H_{ds}$ values of $Na_2Nb_2O_6 \cdot H_2O$ and its dehydrated microporous ($Na_2Nb_2O_6$) and perovskite ($NaNbO_3$) phases (Table 4), the enthalpies of dehydration of $Na_2Nb_2O_6 \cdot H_2O$ with respect to the dehydrated microporous phase and the perovskite at room temperature can be calculated via the thermochemical cycles listed in Table 7.

The enthalpy for the dehydration reaction

$$Na_2Nb_2O_6 \cdot H_2O\ (s, 298\ K) \rightarrow Na_2Nb_2O_6\ (microporous, 298\ K) + H_2O\ (l, 298\ K) \quad (14)$$

is endothermic (46.2 ± 3.6 kJ/mol), whereas that for the reaction

$$Na_2Nb_2O_6 \cdot H_2O\ (s, 298\ K) \rightarrow 2NaNbO_3\ (perovskite, 298\ K) + H_2O\ (l, 298\ K) \quad (18)$$

is exothermic (−21.2 ± 2.7 kJ/mol).

**Table 6. Thermochemical Cycles Used for Calculations of the Standard Enthalpies of Formation of $Na_2Nb_2O_6 \cdot H_2O$**

| enthalpy of formation of $Na_2Nb_2O_6 \cdot H_2O$ from the oxides at 298 K | | |
|---|---|---|
| $Na_2O$ (s, 298 K) → $Na_2O$ (soln, 974 K) | (1) | $\Delta H_1$ |
| $Nb_2O_5$ (s, 298 K) → $Nb_2O_5$ (soln, 974 K) | (2) | $\Delta H_2$ |
| $H_2O$ (l, 298 K) → $H_2O$ (g, 974 K) | (3) | $\Delta H_3$ |
| $Na_2O$ (soln, 974 K) + $Nb_2O_5$ (soln, 974 K) + $H_2O$ (g, 974 K) → $Na_2Nb_2O_6 \cdot H_2O$ (s, 298 K) | (4) | $\Delta H_4$ |
| $Na_2O$ (s, 298 K) + $Nb_2O_5$ (s, 298 K) + $H_2O$ (l, 298 K) → $Na_2Nb_2O_6 \cdot H_2O$ (s, 298 K) | (5) | |
| $\Delta H_{f,ox}^0 = \Delta H_1 + \Delta H_2 + \Delta H_3 + \Delta H_4$ | | |
| **enthalpy of formation of $Na_2Nb_2O_6 \cdot H_2O$ from the elements at 298 K** | | |
| 2Na (s, 298 K) + ($^1/_2$) $O_2$ (g, 298 K) → $Na_2O$ (s, 298 K) | (6) | $\Delta H_6$ |
| 2Nb (s, 298 K) + ($^5/_2$) $O_2$ (g, 298 K) → $Nb_2O_5$ (s, 298 K) | (7) | $\Delta H_7$ |
| $H_2$ (g, 298 K) + ($^1/_2$) $O_2$ (g, 298 K) → $H_2O$ (l, 298 K) | (8) | $\Delta H_8$ |
| $Na_2O$ (s, 298 K) + $Nb_2O_5$ (s, 298 K) + $H_2O$ (l, 298 K) → $Na_2Nb_2O_6 \cdot H_2O$ (s, 298 K) | (9) | $\Delta H_{f,ox}^0$ |
| 2Na (s, 298 K) + 2Nb (s, 298 K) + $H_2$ (g, 298 K) + ($^7/_2$) $O_2$ (g, 298 K) → $Na_2Nb_2O_6 \cdot H_2O$ (s, 298 K) | (10) | |
| $\Delta H_{f,el}^0 = \Delta H_6 + \Delta H_7 + \Delta H_8 + \Delta H_{f,ox}^0$ | | |

**Table 7. Thermochemical Cycles Used for Calculations of the Enthalpies of Dehydration of $Na_2Nb_2O_6 \cdot H_2O$**

| enthalpy of dehydration of $Na_2Nb_2O_6 \cdot H_2O$ with respect to dehydrated microporous phase $Na_2Nb_2O_6$ at 298 K | | |
|---|---|---|
| $Na_2Nb_2O_6 \cdot H_2O$ (s, 298 K) → $Na_2O$ (soln, 974 K) + $Nb_2O_5$ (soln, 974 K) + $H_2O$ (g, 974 K) | (11) | $\Delta H_{11}$ |
| $Na_2O$ (soln, 974 K) + $Nb_2O_5$ (soln, 974 K) → $Na_2Nb_2O_6$ (s, 298 K) | (12) | $\Delta H_{12}$ |
| $H_2O$ (g, 974 K) → $H_2O$ (l, 298 K) | (13) | $\Delta H_{13}$ |
| $Na_2Nb_2O_6 \cdot H_2O$ (s, 298 K) → $Na_2Nb_2O_6$ (s, 298 K) + $H_2O$ (l, 298 K) | (14) | $\Delta H_r$ |
| $\Delta H_r = \Delta H_{11} + \Delta H_{12} + \Delta H_{13}$ | | |
| **enthalpy of dehydration of $Na_2Nb_2O_6 \cdot H_2O$ with respect to $NaNbO_3$ perovskite at 298 K** | | |
| $Na_2Nb_2O_6 \cdot H_2O$ (s, 298 K) → $Na_2O$ (soln, 974 K) + $Nb_2O_5$ (soln, 974 K) + $H_2O$ (g, 974 K) | (15) | $\Delta H_{15}$ |
| $Na_2O$ (soln, 974 K) + $Nb_2O_5$ (soln, 974 K) → 2$NaNbO_3$ (s, 298 K) | (16) | $\Delta H_{16}$ |
| $H_2O$ (g, 974 K) → $H_2O$ (l, 298 K) | (17) | $\Delta H_{17}$ |
| $Na_2Nb_2O_6 \cdot H_2O$ (s, 298 K) → 2$NaNbO_3$ (s, 298 K) + $H_2O$ (l, 298 K) | (18) | $\Delta H_r$ |
| $\Delta H_r = \Delta H_{15} + \Delta H_{16} + \Delta H_{17}$ | | |

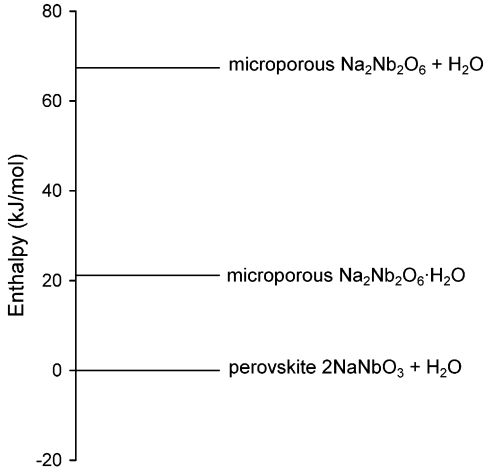


**Figure 5.** Enthalpies of the microporous phase in hydrated ($Na_2Nb_2O_6 \cdot H_2O$) and dehydrated ($Na_2Nb_2O_6$) forms relative to $NaNbO_3$ perovskite (and water).

To facilitate the stability comparison, a diagram showing the relative enthalpies of (1) microporous phase $Na_2Nb_2O_6 \cdot H_2O$, (2) dehydrated microporous phase $Na_2Nb_2O_6$, and (3) $NaNbO_3$ perovskite, is drawn (Figure 5). Microporous $Na_2Nb_2O_6 \cdot H_2O$ is less stable in enthalpy relative to the mixture of $NaNbO_3$ perovskite and liquid water but more stable than that of microporous $Na_2Nb_2O_6$ and water. The enthalpy of dehydration of $Na_2Nb_2O_6 \cdot H_2O$ with respect to the dehydrated microporous phase (reaction 14; $46.2 \pm 3.6$ kJ/mol) is larger than the dehydration enthalpies reported for aluminosilicate zeolites per mole of $H_2O$ (15−40 kJ/mol).[21] This behavior suggests that $H_2O$ in $Na_2Nb_2O_6 \cdot H_2O$ is somewhat more tightly bonded to Na compared to that in zeolites. In this structure, water molecules coordinate not only the extraframework Na [Na(3)] but also the framework Na [Na(1)], rather than sitting loosely in the channels, as in a zeolite. Moreover, the amount of water per mole of hydrated Na ($H_2O/Na = 0.5$) in $Na_2Nb_2O_6 \cdot H_2O$ is significantly smaller than the molar ratio of water to extraframework cations ($\geq 1$) in most zeolites. These structural characteristics may all contribute to the higher hydration/dehydration enthalpy of $Na_2Nb_2O_6 \cdot H_2O$. As shown in Figure 5, the enthalpy of the transition from the dehydrated microporous to perovskite phase at room temperature is $-33.7 \pm 1.6$ kJ per mole of $NaNbO_3$. This value is comparable with that of the transition occurring at ~755 K ($-28.9 \pm 2.2$ kJ/mol), measured using DSC. Their small difference may be attributed to the slight differences in heat capacity between the dehydrated microporous and perovskite phases from 298 to 755 K and any small systematic errors associated with the two different calorimetric techniques (not included in the standard deviations).

The less favorable enthalpy of microporous $Na_2Nb_2O_6 \cdot H_2O$ relative to the mixture of $NaNbO_3$ perovskite and water is consistent with our synthesis. We found that longer reaction time tends to yield more perovskite phase. In other words, pure $Na_2Nb_2O_6 \cdot H_2O$ is probably metastable and can only exist within a narrow window of reaction time. Although our hydrothermal synthesis was conducted at 448 K, the enthalpy for reaction 18 at this temperature should not be significantly different from that at room temperature. Moreover, as water molecules in the solution have more degrees of freedom, the release of water from $Na_2Nb_2O_6 \cdot H_2O$ increases the entropy. Therefore, both enthalpy and entropy favor this dehydration reaction, and the formation of $Na_2Nb_2O_6 \cdot H_2O$ at low temperatures is largely controlled by kinetic factors.

The thermodynamic instability of microporous $Na_2Nb_2O_6 \cdot H_2O$ with respect to $NaNbO_3$ perovskite plus water may be attributed to its energetically unfavorable bonding configurations. In particular, [$NbO_6$] octahedra in $Na_2Nb_2O_6 \cdot H_2O$ form double chains via edge sharing, resulting in oxygen atoms (O1) that each are linked to four Nb cations as the nearest neighbors. This structural arrangement is energetically very unfavorable, because O1 is strongly overbonded (net oxygen charge = 1.33). In contrast, [$NbO_6$] octahedra in $NaNbO_3$ perovskite are corner-linked, where each O is bonded to 2 Nb atoms, resulting in a net oxygen charge of −0.33. This slightly negative charge for the framework O can even be compensated by its bonding, though relatively weak, to the interstitial Na. Thus, O in $NaNbO_3$ perovskite has a net charge close to zero, and this bonding configuration is more stable than that in the microporous structure.

As described earlier, Ti or Zr can replace Nb in the $Na_2Nb_2O_6 \cdot H_2O$ structure via the substitution $M^{4+} + OH^- \rightarrow Nb^{5+} + O^{2-}$ (M = Ti, Zr), forming a solid solution series, $Na_2Nb_{2-x}M_xO_{6-x}(OH)_x \cdot H_2O$. The stability relations of these substituted phases versus their perovskite counterparts are complicated by a number of structural factors related to the substitution, such as hydroxylation and M/Nb cation order−disorder. The crystal chemistry and thermodynamics of the whole solid solution series, as well as the implications for its application in the radioactive Sr disposal, will be the subject of a separate paper.

## Conclusions

A new microporous phase, $Na_2Nb_2O_6 \cdot H_2O$, has been synthesized using the hydrothermal method. In this structure, [$NbO_6$] and [$NaO_6$] octahedra are linked, via edge- and corner-sharing, into a three-dimensional framework. The remaining Na cations occupy the channel sites in a distorted, square-planar coordination. This structure serves as the prototype for the recently synthesized Sandia octahedral molecular sieves (SOMS) family, $Na_2Nb_{2-x}M_xO_{6-x}(OH)_x \cdot H_2O$ (M = Ti, Zr), in which the charge-coupled substitution $M^{4+} + OH^- \rightarrow Nb^{5+} + O^{2-}$ occurs. On heating, $Na_2Nb_2O_6 \cdot H_2O$ first

(16) Tessier, F.; Navrotsky, A.; Le Sauze, A.; Marchand, R. *Chem. Mater.* **2000**, *12*, 148.
(17) Pozdnyakova, I.; Navrotsky, A.; Shilkina, L.; Reznichenko, L. *J. Am. Ceram. Soc.* **2002**, *85*, 379.
(18) Robie, R. A.; Hemingway, B. S. *Thermodynamic Properties of Minerals and Related Substances at 298.15 K and 1 Bar ($10^5$ Pascals) Pressure and at Higher Temperatures*; U.S. Geological Survey Bulletin No. 2131; U.S. Government Printing Office: Washington, DC, 1995.
(19) Chase, M. W., Jr. *NIST-JANAF Thermochemical Tables, 4th ed.*; Journal of Physical and Chemical Reference Data, Monograph No. 9; American Chemical Society: Washington, DC, 1998.
(20) Xu, H.; Su, Y.; Balmer, M. L.; Navrotsky, A. *Chem. Mater.* **2003**, *15*, 1872.
(21) Shim, S. H.; Navrotsky, A.; Gaffney, T. R.; McDougall, J. *Am. Mineral.* **1999**, *84*, 1870.

becomes dehydrated, while maintaining its framework topology, and then converts to $NaNbO_3$ perovskite. Enthalpies of formation of $Na_2Nb_2O_6 \cdot H_2O$ and its dehydrated microporous ($Na_2Nb_2O_6$) and perovskite ($NaNbO_3$) phases from their constituent oxides and elements have been measured using high-temperature drop-solution calorimetry into $3Na_2O \cdot 4MoO_3$ solvent at 974 K. Moreover, the enthalpies of the dehydration reactions, $Na_2Nb_2O_6 \cdot H_2O \rightarrow Na_2Nb_2O_6$ (microporous) + $H_2O$ and $Na_2Nb_2O_6 \cdot H_2O \rightarrow 2NaNbO_3$ (perovskite) + $H_2O$, at room temperature are determined to be $46.2 \pm 3.6$ and $-21.2 \pm 2.7$ kJ/mol, respectively. The exothermic enthalpy for the latter reaction suggests that $NaNbO_3$ perovskite is energetically favorable and that the microporous phase $Na_2Nb_2O_6 \cdot H_2O$ is metastable even under its synthesis conditions. This stability relation is consistent with the ease of conversion of the microporous phase to its perovskite counterpart upon extensive heating.

**Acknowledgment.** We thank S. Vogel and D. Williams for the neutron data collection, P. Yu for the $^{23}Na$ MAS NMR experiment, and Y. Lee and S. Ushakov for assistance with the synchrotron X-ray measurements. This work was supported by the U.S. Department of Energy (DOE) Environmental Management Science Program (EMSP) (Grant FG07-97ER45674). Synchrotron X-ray diffraction was carried out at the National Synchrotron Light Source, Brookhaven National Laboratory, and neutron diffraction was performed at the Manuel Lujan, Jr. Neutron Scattering Center, Los Alamos National Laboratory, both of which are supported by DOE. Sample synthesis was conducted at Sandia National Laboratories. Sandia is a multiprogram laboratory operated by Sandia Corporation, a Lockheed Martin Company, for DOE's National Nuclear Security Administration under contract DE-AC04-94AL85000.

CM035066I